



Published in final edited form as:

Prostaglandins Other Lipid Mediat. 2019 October ; 144: 106353. doi:10.1016/j.prostaglandins.2019.106353.

THE EFFECT OF THE EP3 ANTAGONIST DG-041 ON MALE MICE WITH DIET-INDUCED OBESITY

Ryan P. Ceddia³, Jason D. Downey³, Ryan D. Morrison^{3,5}, Maria P. Kraemer⁴, Sarah E Davis², Jing Wu³, Craig W. Lindsley^{3,5,6}, Huiyong Yin⁷, J. Scott Daniels^{3,5}, Richard M. Breyer^{1,2,3,4}

¹Department of Veterans Affairs, Tennessee Valley Health Authority, Nashville, TN 37232, USA

²Department of Medicine, Division of Nephrology and Hypertension, Vanderbilt University Medical Center, Nashville, TN 37232, USA

³Department of Pharmacology, Vanderbilt University Medical Center, Nashville, TN 37232, USA

⁴Department of Biochemistry, Vanderbilt University Medical Center, Nashville, TN 37232, USA

⁵Vanderbilt Center for Neuroscience Drug Discovery, Vanderbilt University School of Medicine, Nashville, TN 37232, USA

⁶Department of Chemistry, Vanderbilt University, Nashville, TN 37232, USA

⁷Division of Clinical Pharmacology, Vanderbilt University Medical Center, Nashville, TN 37232, USA

Abstract

Background/Aims: The prostaglandin E₂ (PGE₂) EP3 receptor has a multifaceted role in metabolism. Drugs targeting EP3 have been proposed as therapeutics for diabetes; however, studies utilizing global EP3 knockout mice suggest that EP3 blockade increases obesity and insulin resistance. The present studies attempt to determine the effect of acute EP3 antagonist treatment on the diabetic phenotype.

Methods: DG-041 was confirmed to be a high affinity antagonist at the mouse EP3 receptor by competition radioligand binding and by blockade of EP3-mediated responses. DG-041 pharmacokinetic studies were performed to determine the most efficacious route of administration. Male C57BL/6×BALB/c (CB6F1) mice were fed diets containing 10%, 45%, or 60% calories

Corresponding author and person to whom reprints should be addressed: Richard M. Breyer, Ph.D., VA Tennessee Valley Healthcare System, Research and Development 151, ACRE Building F-427, 1310 24th Ave South, Nashville, TN 37212, Tel: 615-873-6842, rich.breyer@vumc.org.

Ryan P. Ceddia, Current Address: Department of Medicine, Division of Cardiovascular Medicine, Vanderbilt University Medical Center, Nashville, TN 37232, USA

Jason D. Downey, Current Address: Leidos Biomedical Research, Frederick, MD, 21703, USA

Maria P. Kraemer, Current Address: University of Kentucky, Lexington, KY, 40506, USA

Jing Wu, Current Address: Department of Pharmacology, Carver College of Medicine, The University of Iowa, Iowa City, IA, 52242, USA

Huiyong Yin, Current Address: Shanghai Institutes for Biological Sciences, Chinese Academy of Sciences, Shanghai, China 200031

Publisher's Disclaimer: This is a PDF file of an unedited manuscript that has been accepted for publication. As a service to our customers we are providing this early version of the manuscript. The manuscript will undergo copyediting, typesetting, and review of the resulting proof before it is published in its final citable form. Please note that during the production process errors may be discovered which could affect the content, and all legal disclaimers that apply to the journal pertain.

from fat to induce obesity. Changes to the metabolic phenotype in these mice were evaluated after one week treatment with DG-041.

Results: Subcutaneous injections of DG-041 at 20 mg/kg blocked the sulprostone-evoked rise in mean arterial pressure confirming the efficacy of this administration regime. Seven day treatment with DG-041 had minimal effect on body composition or glycemic control. DG-041 administration caused a reduction in skeletal muscle triglyceride content while showing a trend toward increased hepatic triglycerides.

Conclusion: Short term EP3 administration of DG-041 produced effective blockade of the EP3 receptor and decreased skeletal muscle triglyceride content but had no significant effects on the diabetic phenotype.

Keywords

Prostaglandin E₂; *Ptger3*; GPCR; pharmacokinetics; ligand binding; obesity; diabetes; metabolic syndrome

Introduction

Obesity, diabetes, and metabolic syndrome, are reaching epidemic proportions worldwide significantly raising health care costs and presenting a tremendous toll on patients and the healthcare system [1]. The exploitation of prostaglandin (PG) signaling pathways to treat these diseases has seen a surge of interest in the last several years. PGs exert their effects by activating specific G-protein coupled receptors (GPCRs) [2, 3]. The use of E prostanoid receptor 3 (EP3) antagonists to promote glucose stimulated insulin secretion (GSIS) from pancreatic islets has been proposed [4] as has the use of EP2 and EP4 agonists to ameliorate type 1 diabetes progression [5]. Additionally, PGI₂ analogs have been shown to have protective effects against obesity- and diabetes-related pathologies including glucose intolerance, nephropathy, and hepatic steatosis [6, 7]. In addition to effects on pancreatic islets and glucose homeostasis, novel roles of prostaglandins have been reported in studies demonstrating an effect of prostaglandins on metabolic fuel utilization, lipolysis, and adipocyte browning [8–11]. Antagonists targeting the EP3 receptor have been of particular interest due to their reported benefits of increasing GSIS [4, 12] and β -cell proliferation [13, 14].

These reports of increased GSIS due to EP3 antagonism prompted us to examine the consequences of developing obesity in the setting of global EP3 gene deletion [14]. Through these studies we demonstrated that EP3^{-/-} mice differ in their response to diet-induced obesity as compared to wild-type mice. EP3^{-/-} mice are more susceptible to diet-induced obesity, have elevated fasting insulin, and have increased β -cell proliferation, which are all the result of an interaction between the EP3 genotype and dietary fat [14]. EP3^{-/-} mice become obese and hyperinsulinemic only when fed a high fat diet (HFD); but when maintained on control or chow diets, EP3^{-/-} mice have normal body weights and phenotypes. In addition to becoming more obese, EP3^{-/-} mice have increased lipolysis and cell death in adipose tissue causing a redistribution of lipid to ectopic tissues and insulin

resistance [14]. This suggests that the purported benefits of increasing GSIS may be negated by increased insulin resistance.

These effects of EP3 on the metabolic phenotype in the aforementioned study were noted in a model of chronic EP3 disruption, utilizing mice that had a global EP3 gene deletion since birth [14]. This earlier study did not investigate the consequences of EP3 disruption in mice that were obese prior to the EP3 loss, akin to what would occur in a therapeutic setting. The use of an EP3 antagonist may be most useful in type 2 diabetics, as Kimple *et al.* reported that the EP3 antagonist L-798,106 improves GSIS only in islets from BTBR-*Lep^{ob/ob}* mice and diabetic individuals [4].

In order to determine if acute inhibition of EP3 affects glucose homeostasis and/or insulin sensitivity in obese mice, the EP3 antagonist DG-041 [15] was administered to wild-type mice with both moderate and severe diet-induced obesity for one week and changes in insulin sensitivity, body weight, and ectopic lipid distribution were assessed. Prior to initiating these studies, we confirmed that DG-041 is a high-affinity, functional antagonist of the mouse EP3 receptor and determined the optimal route of administration to ensure that the plasma concentrations of DG-041 would provide an adequate blockade of the receptor. This short-term DG-041 administration had no effect on body weight or composition and did not have a significant effect on HOMA-IR. Interestingly, this short-term treatment with DG-041 caused a reduction in skeletal muscle triglyceride content while showing a trend toward increased hepatic triglycerides, which is consistent with inhibition of hepatic triglyceride secretion or altered triglyceride clearance.

Materials & Methods

Materials

HEK293 cells were purchased from ATCC (#CRL-1573, Manassas, VA). LVIP2.0Zc cells were a generous gift of Michael Brownstein [16]. PGE₂ and sulprostone were purchased from Cayman Chemical (Ann Arbor, MI). [³H] PGE₂ was purchased from Perkin Elmer (Waltham, MA). Indomethacin and sodium butyrate were purchased from Sigma Aldrich (St. Louis, MO). High-glucose, no L-glutamine Dulbecco's Modified Eagle Medium (DMEM), OptiMEM I, and Lipofectamine 2000 were purchased from Invitrogen (Carlsbad, CA). L-glutamine and penicillin/streptomycin were purchased from MediaTech (Manassas, VA). Fetal bovine serum (FBS) was purchased from Atlanta Biologicals (Lawrenceville, GA). DG-041 synthesis [15] and its DMPK profile were provided by the Vanderbilt Institute of Chemical Biology Synthesis Core, Vanderbilt University, Nashville, TN 37232-0412.

Cell Culture

Cells were maintained at 37 °C / 5% CO₂ in DMEM supplemented with 10 % FBS, 2 mM L-glutamine, 100 units/mL penicillin, and 100 µg/mL streptomycin. For cell membrane / receptor preparations, HEK293 cells were transiently transfected with a previously described EP3γ cDNA plasmid [17] that contained a single threonine-to-serine variant from published sequence [18] which appears to have no effect on receptor function.

LVIP2.0Zc cell culture medium also contained 300 µg/mL hygromycin B to maintain integration of vasointestinal peptide (VIP) / *lacZ* reporter plasmid [16]. LVIP2.0Zc cells stably expressing N-terminal HA-tagged mouse EP3γ receptor [18] were generated by transfection of a pcDNA3 plasmid containing receptor cDNA and neomycin resistance cassette. A monoclonal HAmEP3γ-expressing LVIP2.0Zc cell line was generated by limiting dilution method. Incubating in 500 µg/mL G418 in addition to hygromycin allowed for maintenance of double transformants. Twenty-four hours prior to performing CRE assays, HAmEP3γ-expressing LVIP2.0Zc cells were plated in 96-well plates at a density of 5×10^5 cells per well in 100 µL of complete DMEM containing 20 µM indomethacin.

Competition Radioligand Binding

Total cell membranes from HEK293 transfectants described above were prepared as described [19]. Membranes (5 – 10 µg) were incubated with [³H] PGE₂ (5 nM) and a range of concentrations of unlabeled test compound (1 nM – 10 µM) in 200 µL of binding buffer (25 mM potassium phosphate, 1 mM EDTA, and 10 mM MgCl₂, pH 6.2) for 1 hour at 30 °C. Excess PGE₂ (10 µM) was used as a control to determine non-specific radioligand binding. Binding reactions were terminated by vacuum filtration of glass fiber filters and radioactivity was quantified as previously described [19].

CRE/LacZ Reporter Assay

LVIP2.0Zc cells in 96-well plates stably expressing the HAmEP3γ receptor were incubated with sulprostone (1 pM – 0.1 µM) and DG-041 (0.1 nM – 10 nM) in Opti-MEM containing 5 mM sodium butyrate and 20 mM indomethacin. After cells were stimulated for 6 hours, media was aspirated and cells were washed with PBS. Cells were incubated for 10 minutes at room temperature in 25 µL of lysis buffer (10 mM sodium phosphate, 0.2 mM MgSO₄, and 10 mM MnCl₂, pH 8.0). Assay plates were developed as described [20]. Concentration response curves to sulprostone in the presence of varying amounts of DG-041 were determined by measuring relative enzyme activity as absorbance at 570 nm on Multiskan Ascent plate reader (Thermo Labsystems, Waltham, MA). Data were analyzed in the method of Schild [21].

In vivo pharmacokinetics

For pharmacokinetics studies, all mice were maintained on a standard chow diet (Laboratory Rodent Diet 5001, LabDiet). Male C57BL/6J mice were administered 30 mg/kg DG-041 in corn oil (200 µL) by mouth (*per os*, PO) via gavage at time $t = 0$. At 20 min, 45 min, 90 min, 3, 6, 12, and 24 hours mice were euthanized in pairs by isoflurane overdose, blood was collected by cardiac puncture into syringes containing 3.8 % sodium citrate, and DG-041 concentration determined by LC/MS/MS.

Male C57BL/6 mice were administered 100 µL of 2 mg/kg DG-041 by intravenous (IV) tail vein injection or 20 mg/kg DG-041 by subcutaneous (SC) injection. For IV injections, DG-041 was dissolved in one part PEG400 and one part 0.9% saline. For SC injections, DG-041 was dissolved in DMSO, and was then diluted to one part DMSO, six parts PEG400, and 3 parts 0.9% saline. Blood was collected for plasma isolation by saphenous vein blood draw into EDTA coated tubes (Sarstedt, Nümbrecht, Germany) for the first five

time points, with the final blood draw being obtained by cardiac puncture in euthanized mice. Plasma was stored at -80°C until LC/MS/MS analysis.

Analyte was extracted by precipitation with an ice-cold solution of internal standard in acetonitrile, followed by centrifugation at $3000 \times g$ at 4°C for 10 minutes. Samples were incubated on ice for 5 minutes until organic-aqueous phase interface was apparent. An aliquot of the organic phase (750 μL) was transferred to a clean tube, dried at 30°C under nitrogen, and reconstituted in 85:15 water:acetonitrile (125 μL). Samples were analyzed by LC/MS/MS. Test compound plasma concentrations were calculated by comparing the ratio of analyte mass spectrometer response AUC to internal standard mass spectrometer response AUC to a calibration curve of known analyte concentration analyte AUC:standard AUC values.

Internal carotid blood pressure measurements

Male wild-type C57BL/6 mice, age 12 to 16 weeks and 20 to 25 g in body weight, had a jugular and carotid catheter inserted and were allowed to recover from surgery for five to seven days. On the day of the study, mice received a 100 μL total volume, SC injection of either 20 mg/kg DG-041 or vehicle. Mice were then anesthetized with 80 mg/kg ketamine (Fort Dodge Laboratories, Fort Dodge, IA) and 8 mg/kg inactin (BYK, Germany) via intraperitoneal administration. Blood pressure was measured with a Cobe CDX II transducer connected to a blood pressure analyzer (Blood Pressure Analyzer™ 400, Micro-Med, Louisville, KY) as previously described [22]. Sulprostone was mixed with 25 μL of saline and injected as a bolus via the jugular catheter over 20 seconds. Blood pressures, including systolic, diastolic, and mean arterial pressure (MAP), and heart rates were recorded at 10 second intervals.

Diet induced obesity

Mice utilized for diet-induced obesity studies were male CB6F1/J mice (Jackson Laboratories Stock #100007) which are the F1 generation of a cross between male C57BL/6 and female Balb/c. Mice were obtained at three weeks of age, housed at Vanderbilt for three days on the standard chow diet after which time they were fed either control (10% calories from fat; 4.3% fat by weight, D12450Bi, Research Diets, New Brunswick, NJ), HFD (45% calories from fat; 24% fat by weight, D12451i, Research Diets), or very high fat diet (VHFD) (60% calories from fat; 34.9% fat by weight, D12492i, Research Diets). Mice were maintained on a 12-hour light/dark cycle and housed with three to five animals per cage on corncob bedding except during fasting when placed on Pure-o'Ceil™ bedding (The Andersons, Maumee, OH). Mice were weighed weekly and body composition was assessed every four weeks by pulsed NMR (Bruker Instruments, The Woodlands, TX) at the Vanderbilt Mouse Metabolic Phenotyping Center. After 17 weeks of defined diet feeding, mice were injected via SC with 20 mg/kg DG-041 or vehicle twice daily for one week. At the termination of the experiment, mice were euthanized by isoflurane overdose and liver, epididymal fat pads, and skeletal muscle were dissected. All procedures were approved by the Institutional Animal Care and Use Committee at Vanderbilt University.

Assessment of insulin resistance

At the end of the feeding study, mice were fasted for 6 hours during the light cycle. EDTA plasma was collected by saphenous vein blood draw and insulin was quantified by radioimmunoassay at the Vanderbilt Hormone Assay Core. Blood glucose was measured in the saphenous vein blood with an Accu-Check Aviva glucometer and glucose test strips (Roche Diagnostics). HOMA-IR was calculated as the fasting insulin level ($\mu\text{U}/\text{mL}$) \times blood glucose level (mg/dL) / 405.

Histology

Livers were fixed in 10% formaldehyde overnight at 4°C and subsequently stored in 70% ethanol at 4°C prior to paraffin embedding and hematoxylin and eosin (H&E) staining. For Oil Red O (ORO) staining, liver samples were fixed by freezing in Tissue-Tek OCT medium. Histology was performed by the Vanderbilt Translational Pathology Shared Resource. All slides were imaged at 20 \times with a Leica SCN400 Slide Scanner by the Vanderbilt Digital Histology Shared Resource.

Tissue fatty acid composition

Lipids were extracted from ~100 mg flash frozen liver or combined gastrocnemius and soleus skeletal muscle tissue [23]. The extracts were filtered, and lipids were extracted using two-phase liquid extraction acetonitrile/chloroform. Lipids were separated by thin layer chromatography using Silica Gel 60 A plates developed in petroleum ether, ethyl ether, acetic acid (80:20:1) and visualized by rhodamine 6G. Phospholipids, diglycerides, triglycerides and cholesteryl esters were scraped from the plates and methylated using $\text{BF}_3/\text{methanol}$ [24]. The methylated fatty acids were extracted and analyzed by gas chromatography. Gas chromatographic analyses were carried out on an Agilent 7890A gas chromatograph equipped with flame ionization detectors and a capillary column (SP2380, Supelco, Bellefonte, PA). Helium was used as a carrier gas. Fatty acid methyl esters were identified by comparing the retention times to those of known standards. Triglycerides were quantified by the Mouse Metabolic Phenotyping Center Lipid Lab.

Statistics

Data were analyzed using GraphPad Prism (GraphPad Software, La Jolla, CA). Change in mean arterial pressure was analyzed with an unpaired t-test. Studies examining the effect of different diets without drug treatment were analyzed with a 1-way ANOVA using a Bonferroni multiple comparisons test comparing the mean of each group to the mean of every other group. For studies comparing mice before and after drug treatment, genotype \times diet groups were compared before and after DG-041 or vehicle treatment using a 2-way ANOVA with repeated measures. Terminal studies without pre-drug treatment data were analyzed with a 2-way ANOVA comparing drug treatment versus diet. Multiple comparison tests for all 2-way ANOVAs were performed with the Bonferroni correction for DG-041 treatment only and are indicated on figures by asterisks corresponding to * $P < 0.05$, ** $P < 0.01$, *** $P < 0.001$. For all studies, $P < 0.05$ was considered statistically significant.

Results

DG-041 is a high affinity ligand for the mouse EP3 receptor

DG-041 demonstrated high affinity binding to the mouse EP3 receptor in competitive radioligand binding assays, competing against [³H]PGE₂ for binding sites in HEK293 membranes overexpressing mouse EP3 receptors. Prior studies have reported that the kinetics of DG-041 binding to the human EP3 receptor are characterized by slow, tight binding [25, 26]; on the time scale of the *in vitro* binding assays (a few hours) utilized in these studies, DG-041 is therefore predicted to behave as a pseudo-irreversible ligand of the mouse EP3 receptor. An apparent affinity constant of $pK_i = 9.2 \pm 0.1$ and pIC_{50} of 8.7 ± 0.1 of DG-041 for the mouse EP3 receptor was observed (Figure 1A).

In the LVIP2.0Zc-based CRE/LacZ assay [16] mEP3 γ behaved as a classical G_i-coupled receptor (Figure 1B), as opposed to its stimulatory behavior in the CRE assay employing transiently pCRE/LacZ-transfected HEK293 cells [17]. LVIP2.0Zc cells were stimulated with isoproterenol, activating the β_2 adrenergic receptors and raising cAMP levels. Activation of mEP3 γ potently suppressed expression of the reporter indicating a reduction in intracellular cAMP. Blockade of the mouse EP3 γ receptor by DG-041 was characterized using the method of Schild [21]. Picomolar concentrations of DG-041 right-shifted the concentration response curve to sulprostone, and DG-041 completely suppressed signaling through the EP3 receptor at low nanomolar concentrations (Figure 1B, left). DG-041 was found to be a high-affinity, functional antagonist of the mouse EP3 γ receptor ($pK_D = 10.85$, $m = 0.72$; Figure 1B, right). The affinity of DG-041 binding to the mouse EP3 receptor observed in these studies is similar to that observed in previous studies on the human EP3 receptor [25].

In vivo pharmacokinetics of DG-041

To determine the *in vivo* pharmacokinetics of DG-041, multiple routes of administration were assessed. When DG-041 was administered to male C57BL/6 mice at a dose of 30 mg/kg *per os* (PO) it reached a maximum plasma concentration of 721 (\pm 612) nM. It was rapidly eliminated and plasma concentrations of DG-041 dropped below the lower limit of detection after 3 hours (Figure 2A). Noncompartmental analysis of the plasma concentration-time profile revealed $t_{1/2}$ for DG-041 in mice of 1.23 hours.

DG-041 was administered by IV tail vein injection to male C57BL/6 mice at a dose of 2 mg/kg and achieved an initial plasma concentration of 1246 nM (\pm 718) (Figure 2B). These data indicate that administration of DG-041 by either PO or IV injection would be impractical for longer exposure studies due to its short half-life.

SC injection was investigated as an alternate means of administering DG-041. DG-041 was administered to male C57BL/6 mice at 20 mg/kg and achieved a maximum plasma concentration of 1385 nM (\pm 716) at 1 hour displaying an average AUC of 331.4 nM·h over the 26-hour period (Figure 2C). The slower rate of drug absorption associated with SC administration allowed the plasma concentrations of DG-041 to remain evident throughout the 26-hour period. We and others have reported that global EP3 knockout predisposes mice to obesity [14, 27]. To limit effects on feeding behavior and locomotor activity, recent efforts

to optimize EP3 antagonists have attempted to limit brain exposure [28]. However, previous studies had not determined whether or not DG-041 crosses the blood-brain barrier. Therefore, we measured the DG-041 concentration in the brain of one SC injected mouse from each of the 1-, 4-, and 8-hour time points. DG-041 was found in all three mouse brains indicating that it crosses the blood-brain barrier (Figure 2D).

DG-041 antagonism of EP3 *in vivo* was confirmed by its ability to block the vasopressor effects of the EP3/EP1 agonist, sulprostone. Vehicle or 20 mg/kg DG-041 was administered by SC injection two hours prior to internal carotid blood pressure measurements. Following the measurement of baseline blood pressure, 10 µg/kg sulprostone was administered IV via the jugular catheter which caused a rise in mean arterial pressure (MAP) in vehicle treated mice (Figure 2E). We have previously shown that sulprostone and other EP3 agonists cause a rise in MAP [22, 29, 30]. The DG-041 treatment effectively blocked the sulprostone-evoked change in MAP (Figure 2E). In subsequent studies DG-041 was administered via SC injections at 20 mg/kg twice daily, which would provide plasma concentrations sufficient to achieve full coverage of the EP3 receptors.

CB6F1 mice are obese when fed a HFD

CB6F1 male mice were fed HFD (45% calories from fat), VHFD (60% calories from fat) or a micronutrient matched control diet (10% calories from fat). Body weight increased in each of the three groups over the course of the study (Figure 3A). Body weight in both HFD and VHFD fed mice increased at a greater rate than in animals fed control diet, with a divergence in body weight becoming apparent between six and eleven weeks of age. Body composition analyses over the course of the study revealed that fat mass also increased with age and dietary fat (Figure 3B). In addition, dietary fat also had a significant effect on the lean mass of these mice (Figure 3C).

CB6F1 mice are insulin resistant when fed a HFD

Blood glucose and plasma insulin were measured in CB6F1 mice after 17 weeks of control diet, HFD, or VHFD feeding. Regardless of dietary fat content, basal glucose levels in the fasted state showed no differences (Figure 4A). Fasting insulin levels increased with increasing dietary fat (Figure 4B). Insulin resistance, as determined by calculation of the homeostatic model assessment of insulin resistance (HOMA-IR), is increased in CB6F1 mice proportional to the dietary fat content (Figure 4C).

EP3 antagonist does not affect body composition

At 20 weeks of age, CB6F1 mice that had been fed control diet, HFD, or VHFD were administered EP3 antagonist, DG-041, or vehicle for one week by twice-daily SC injections. Body weight decreased in HFD and VHFD fed mice following administration of either DG-041 or vehicle (Figure 5A), suggesting that the observed decreased body weight was due to the vehicle and/or the stress of twice-daily handlings and injections. In these mice, we also observed a concomitant decrease in fat mass (Figure 5B). Lean mass was not significantly altered by DG-041 or vehicle (Figure 5C). DG-041, as compared to vehicle, had no effect on body weight, fat mass, or muscle mass in any dietary treatment group. Higher dietary fat content increased the post-mortem weight of the liver and epididymal fat

pads (Figure 6). Liver and epididymal fat pad masses were not significantly affected by DG-041, except in mice fed control diet where an increase in liver weight was observed (1257.5 ± 104.2 vs. 1801.8 ± 76.8 , $P = 0.0047$).

EP3 antagonist does not affect insulin sensitivity

Blood glucose and plasma insulin were measured in 6-hour fasted CB6F1 mice following a week of DG-041 or vehicle injections. Vehicle and DG-041 treatments produced similar changes in blood glucose and plasma insulin concentrations, as compared to the individuals' levels the week before treatments began (Figure 7A,B). Consequently, HOMA-IR was unaffected by DG-041 (Figure 7C).

EP3 antagonist decreases skeletal muscle triglycerides

EP3^{-/-} mice have increased insulin resistance when fed a HFD due to ectopic lipid accumulation in their liver and skeletal muscle [14]. In order to assess whether short-term EP3 blockade with DG-041 would similarly affect ectopic lipid accumulation in mice with diet-induced obesity, liver and skeletal muscle triglyceride contents were measured in these CB6F1 mice following vehicle or DG-041 treatment. Dietary fat and DG-041 treatment were both found to affect the fatty acid composition of hepatic and muscle triglycerides (Tables 1 and 2, respectively). Total amounts of triglyceride in both liver and skeletal muscle were increased with increasing dietary fat (Figure 8). Hepatic triglycerides were not significantly altered by DG-041 treatment (Figure 8A); however, within the group of mice fed VHFD, DG-041 treatment displayed a trend toward increased hepatic triglycerides ($P = 0.0625$). The liver histology generally parallels the triglyceride quantification (Figure 9). Hepatic steatosis and lipid staining with Oil Red O (ORO) were increased in mice fed HFD and VHFD. DG-041 treatment appeared to increase cytoplasmic volume and ORO staining in mice fed VHFD. DG-041 caused a marked reduction in the amount of triglyceride in skeletal muscle (Figure 8B). This decrease was especially noticeable in the mice that were fed VHFD ($P < 0.001$).

Discussion

In the present studies, we examined the consequences of acute EP3 blockade with DG-041 in a setting of diet-induced obesity. DG-041 is one of the most advanced small molecule antagonists of the EP3 receptor, having progressed to phase II clinical trials [31]. First, we confirmed that DG-041 acts as a high affinity antagonist of the mouse EP3 receptor. We then determined that SC administration of DG-041 provides adequate coverage in contrast to IV or PO where rapid clearance and poor bioavailability were observed. Our estimates of time with adequate DG-041 coverage *in vivo* are likely conservative due to the slow tight binding of this compound [26]. Finally, we administered DG-041 for one week to CB6F1 mice with moderate and severe diet-induced obesity to characterize its effect on body weight, glucose homeostasis, and lipid distribution.

We chose to utilize CB6F1 mice for the metabolic phenotyping studies because conventional inbred strains of mice lack heterozygosity, which is endemic in humans. To our knowledge, there are no other studies characterizing the effects of high fat diet on CB6F1 mice, though

the parental strains of CB6F1 mice, C57BL/6 and Balb/c, are very well characterized and exhibit a strikingly different phenotype. C57BL/6 mice are more prone to obesity than Balb/c [32], while Balb/c mice have more severe HFD-induced hepatic lipid accumulation [33–35]. We found that CB6F1 mice are susceptible to diet-induced obesity and insulin resistance; in fact, they consistently weighed more than C57BL/6 mice in our previous studies [14]. This is likely due to hybrid vigor of the CB6F1 mice, although the differences due to maternal effects may also influence the phenotype of CB6F1 mice [36–38].

The use of the EP3 antagonist L-798,106 as a therapeutic for diabetes has recently garnered much attention as two studies have demonstrated its ability to enhance GSIS [4, 12], though these findings were not replicable in our lab utilizing islets derived from EP3^{-/-} mice or treated with the EP3 antagonist DG-041 [14]. It is possible that the beneficial effects of EP3 inhibition can only be seen in a setting of obesity as L-798,106 has been reported to only have beneficial effects in islets from diabetic patients or BTBR mice with the Leptin^{ob/ob} mutation [4]. However, another group found that L-798,106 was effective in islets derived from wild-type C57BL/6 mice [12], the same genetic background as we used in our prior studies [14]. In addition to the effects on GSIS, we demonstrated that when fed a HFD, EP3^{-/-} mice develop more severe obesity and have increased adipose tissue inflammation, cell death, and lipolysis resulting in greater ectopic lipid accumulation and insulin resistance than would be expected of an EP3^{+/+} mouse of a similar body mass [14]. Because EP3 blockade has potential therapeutic uses for improving GSIS but also has the adverse side effect of increasing obesity and insulin resistance, we sought to determine if short-term treatment with the small molecule EP3 antagonist, DG-041, has beneficial effects on fasting glucose and insulin and/or detrimental effects on body weight, composition, and lipid distribution.

Two HFDs (45% and 60% calories from fat) were used as models of moderate and severe diet-induced obesity. When compared to vehicle treated mice, DG-041 treatment did not affect blood glucose, plasma insulin, body weight, or insulin sensitivity on either diet. EP3^{-/-} mice fed a HFD have significant lipid redistribution from adipose tissue to skeletal muscle and liver tissue [14]; so, we quantified triglycerides in these tissues following DG-041 treatment. In VHFD fed mice, treatment with DG-041 was associated with elevated hepatic triglycerides, though this did not reach statistical significance. Surprisingly, in these same mice, skeletal muscle triglycerides were markedly decreased in the DG-041 treated cohort, in contrast to our prior observation of increased triglycerides in this same tissue in EP3^{-/-} mice [14]. Loss of skeletal muscle triglycerides in DG-041 treated mice is not associated with the loss of body mass during treatment as both vehicle and DG-041 treated mice lost weight, but only DG-041 treated mice demonstrated decreased skeletal muscle triglycerides. These results are not consistent with lipid redistribution from adipose tissue, such as increased lipolysis or cellular death, which would be expected to result in increased triglycerides in both liver and skeletal muscle [9, 14].

This decrease in skeletal muscle triglycerides may be explained by tissue-specific alterations in lipid uptake or triglyceride metabolism. Increased triglyceride oxidation would be expected to result in a loss of body weight as compared to vehicle control, which was not observed. Decreased lipid uptake in skeletal muscle would also be predicted to reduce

muscle triglycerides. In this case we hypothesize that muscle is sensitive to the action of EP3, whereas liver is not. Consistent with this hypothesis, Yan *et al.* demonstrated that mice with a liver-specific deletion of EP3 have no differences in hepatic triglycerides [39].

These findings highlight the differences between short term antagonist blockade and chronic genetic disruption of the EP3 receptor, where an increase in skeletal muscle triglycerides was observed. In the chronic state, lipid-lowering effects of EP3 loss in skeletal muscle may be overwhelmed by chronic lipid redistribution from adipocytes, especially when cell death limits the ability of adipose tissue to store lipids.

Conclusion

These studies demonstrate that DG-041 is a selective antagonist for the mouse EP3 receptor and may be used pharmacologically in mice to investigate the effects of EP3 blockade on physiological functions *in vivo*. These studies also suggest that EP3 may have a previously unrecognized role in metabolic physiology, particularly in the suppression of lipid accretion in skeletal muscle. Furthermore, they also establish that CB6F1 mice are susceptible to diet-induced obesity and insulin resistance.

Acknowledgements

We thank Prof. Owen McGuinness for helpful discussions. This work was supported by National Institutes of Health grants HL127218 (R.M.B.), HL134895 (R.M.B.), DK46205 (R.M.B.) and DK37097 (R.M.B.). Merit Awards from the Department of Veterans Affairs to R.M.B. (1BX000616) supported this paper. R.P.C. was supported in part by a Graduate Award for Integrative Research in Pharmacology from The American Society for Pharmacology and Experimental Therapeutics and by funding provided by the Vanderbilt Center for Kidney Disease. The authors gratefully acknowledge the use of the surgical and experimental services provided by the Vanderbilt Mouse Metabolic Phenotyping Center (U24DK059637). The Vanderbilt University Hormone Assay & Analytical Services Core was supported by DK020593 and DK059637.

References

- O'Neill S, O'Driscoll L: Metabolic syndrome: a closer look at the growing epidemic and its associated pathologies. *Obes Rev* 2015;16:1–12.
- Breyer RM, Bagdassarian CK, Myers SA, Breyer MD: Prostanoid receptors: subtypes and signaling. *Annu Rev Pharmacol Toxicol* 2001;41:661–690. [PubMed: 11264472]
- Hata AN, Breyer RM: Pharmacology and signaling of prostaglandin receptors: multiple roles in inflammation and immune modulation. *Pharmacol Ther* 2004;103:147–166. [PubMed: 15369681]
- Kimple ME, Keller MP, Rabaglia MR, Pasker RL, Neuman JC, Truchan NA, Brar HK, Attie AD: Prostaglandin E₂ Receptor, EP3, Is Induced in Diabetic Islets and Negatively Regulates Glucose- and Hormone-Stimulated Insulin Secretion. *Diabetes* 2013;62:1904–1912. [PubMed: 23349487]
- Vennemann A, Gerstner A, Kern N, Bouzas NF, Narumiya S, Maruyama T, Nüsing RM: PTGS-2-PTGER2/4 Signaling Pathway Partially Protects From Diabetogenic Toxicity of Streptozotocin in Mice. *Diabetes* 2012;61:1879–1887. [PubMed: 22522619]
- Batchu SN, Majumder S, Bowskill BB, White KE, Advani SL, Brijmohan AS, Liu Y, Thai K, Azizi PM, Lee WL, Advani A: Prostaglandin I₂ Receptor Agonism Preserves β -Cell Function and Attenuates Albuminuria Through Nephron-Dependent Mechanisms. *Diabetes* 2016;65:1398–1409. [PubMed: 26868296]
- Sato N, Kaneko M, Tamura M, Kurumatani H: The prostacyclin analog Beraprost sodium ameliorates characteristics of metabolic syndrome in obese Zucker (fatty) rats. *Diabetes* 2010;59:1092–1100. [PubMed: 20068136]

8. Iyer A, Lim J, Poudyal H, Reid RC, Suen JY, Webster J, Prins JB, Whitehead JP, Fairlie DP, Brown L: An Inhibitor of Phospholipase A₂ Group IIA Modulates Adipocyte Signaling and Protects Against Diet-Induced Metabolic Syndrome in Rats. *Diabetes* 2012;61:2320–2329. [PubMed: 22923652]
9. Jaworski K, Ahmadian M, Duncan RE, Sarkadi-Nagy E, Varady KA, Hellerstein MK, Lee H-Y, Samuel VT, Shulman GI, Kim K-H, de Val S, Kang C, Sul HS: AdPLA ablation increases lipolysis and prevents obesity induced by high-fat feeding or leptin deficiency. *Nat Med* 2009;15:159–168. [PubMed: 19136964]
10. Vegiopoulos A, Müller-Decker K, Strzoda D, Schmitt I, Chichelnitskiy E, Ostertag A, Berriel Diaz M, Rozman J, Hrabe de Angelis M, Nüsing RM, Meyer CW, Wahli W, Klingenspor M, Herzig S: Cyclooxygenase-2 controls energy homeostasis in mice by de novo recruitment of brown adipocytes. *Science* 2010;328:1158–1161. [PubMed: 20448152]
11. Virtue S, Feldmann H, Christian M, Tan CY, Masoodi M, Dale M, Lelliott C, Burling K, Campbell M, Eguchi N, Voshol P, Sethi JK, Parker M, Urade Y, Griffin JL, Cannon B, Vidal-Puig A: A new role for lipocalin prostaglandin D synthase in the regulation of brown adipose tissue substrate utilization. *Diabetes* 2012;61:3139–3147. [PubMed: 22923471]
12. Shridas P, Zahoor L, Forrest KJ, Layne JD, Webb NR: Group X Secretory Phospholipase A₂ Regulates Insulin Secretion Through a Cyclooxygenase-2-Dependent Mechanism. *J Biol Chem* 2014;289:27410–27417. [PubMed: 25122761]
13. Carboneau BA, Allan JA, Townsend SE, Kimple ME, Breyer RM, Gannon M: Opposing effects of prostaglandin E₂ receptors EP₃ and EP₄ on mouse and human β -cell survival and proliferation. *Mol Metab* 2017;6:548–559. [PubMed: 28580285]
14. Ceddia RP, Lee D, Maulis MF, Carboneau BA, Threadgill DW, Poffenberger G, Milne G, Boyd KL, Powers AC, McGuinness OP, Gannon M, Breyer RM: The PGE₂ EP₃ Receptor Regulates Diet-Induced Adiposity in Male Mice. *Endocrinology* 2016;157:220–232. [PubMed: 26485614]
15. Heptinstall S, Espinosa DI, Manolopoulos P, Glenn JR, White AE, Johnson A, Dovlatova N, Fox SC, May JA, Hermann D, Magnusson O, Stefansson K, Hartman D, Gurney M: DG-041 inhibits the EP₃ prostanoid receptor--a new target for inhibition of platelet function in atherothrombotic disease. *Platelets* 2008;19:605–613. [PubMed: 19012178]
16. König M, Mahan LC, Marsg JW, Fink JS, Brownstein MJ: Method for identifying ligands that bind to cloned G_s- or G_i-coupled receptors. *Mol Cell Neurosci* 1991;2:331–337. [PubMed: 19912816]
17. Downey JD, Sanders CR, Breyer RM: Evidence for the presence of a critical disulfide bond in the mouse EP₃ γ receptor. *Prostaglandins Other Lipid Mediat* 2011;94:53–58. [PubMed: 21236356]
18. Irie A, Sugimoto Y, Namba T, Harazono A, Honda A, Watabe A, Negishi M, Narumiya S, Ichikawa A: Third isoform of the prostaglandin-E-receptor EP₃ subtype with different C-terminal tail coupling to both stimulation and inhibition of adenylate cyclaseThird isoform of the prostaglandin-E-receptor EP₃ subtype with different C-terminal tail coupling to both stimulation and inhibition of adenylate cyclase. *Eur J Biochem* 1993;217:313–318. [PubMed: 8223569]
19. Breyer RM, Emeson RB, Tarnag J-L, Breyer MD, Davis LS, Abromson RM, Ferrenbach SM: Alternative splicing generates multiple isoforms of a rabbit prostaglandin E₂ receptor. *J Biol Chem* 1994;269:6163–6169. [PubMed: 8119961]
20. Audoly LP, Ma L, Feoktistov I, de Foe SK, Breyer MD, Breyer RM: Prostaglandin E-prostanoid-3 receptor activation of cyclic AMP response element-mediated gene transcription. *J Pharmacol Exp Ther* 1999;289:140–148. [PubMed: 10086997]
21. Schild HO: pA, a new scale for the measurement of drug antagonism. *British journal of pharmacology and chemotherapy* 1947;2:189–206. [PubMed: 20258355]
22. Zhang Y, Guan Y, Schneider A, Brandon S, Breyer RM, Breyer MD: Characterization of murine vasopressor and vasodepressor prostaglandin E(2) receptors. *Hypertension* 2000;35:1129–1134. [PubMed: 10818076]
23. Folch J, Lees M, Sloane Stanley GH: A simple method for the isolation and purification of total lipids from animal tissues. *J Biol Chem* 1957;226:497–509. [PubMed: 13428781]
24. Morrison WR, Smith LM: Preparation of Fatty Acid Methyl Esters and Dimethylacetals from Lipids with Boron Fluoride--Methanol. *J Lipid Res* 1964;5:600–608. [PubMed: 14221106]

25. Singh J, Zeller W, Zhou N, Hategan G, Mishra RK, Polozov A, Yu P, Onua E, Zhang J, Ramírez JL, Sigthorsson G, Thorsteinnsdottir M, Kiselyov AS, Zembower DE, Andrésón T, Gurney ME: Structure-activity relationship studies leading to the identification of (2E)-3-[1-[(2,4-dichlorophenyl)methyl]-5-fluoro-3-methyl-1H-indol-7-yl]-N-[(4,5-dichloro-2-thienyl)sulfonyl]-2-propenamide (DG-041), a potent and selective prostanoid EP3 receptor antagonist, as a novel antiplatelet agent that does not prolong bleeding. *J Med Chem* 2010;53:18–36. [PubMed: 19957930]
26. Jones RL, Woodward DF, Wang JW, Clark RL: Roles of affinity and lipophilicity in the slow kinetics of prostanoid receptor antagonists on isolated smooth muscle preparations. *Br J Pharmacol* 2011;162:863–879. [PubMed: 20973775]
27. Sanchez-Alavez M, Klein I, Brownell SE, Tabarean IV, Davis CN, Conti B, Bartfai T: Night eating and obesity in the EP3R-deficient mouse. *Proc Natl Acad Sci U S A* 2007;104:3009–3014. [PubMed: 17307874]
28. Lee EC, Futatsugi K, Arcari JT, Bahnck K, Coffey SB, Derksen DR, Kalgutkar AS, Loria PM, Sharma R: Optimization of amide-based EP3 receptor antagonists. *Bioorg Med Chem Lett* 2016;26:2670–2675. [PubMed: 27107947]
29. Chen L, Miao Y, Zhang Y, Dou D, Liu L, Tian X, Yang G, Pu D, Zhang X, Kang J, Gao Y, Wang S, Breyer MD, Wang N, Zhu Y, Huang Y, Breyer RM, Guan Y: Inactivation of the E-prostanoid 3 receptor attenuates the angiotensin II pressor response via decreasing arterial contractility. *Arterioscler Thromb Vasc Biol* 2012;32:3024–3032. [PubMed: 23065824]
30. Downey JD, Saleh SA, Bridges TM, Morrison RD, Daniels JS, Lindsley CW, Breyer RM: Development of an in vivo active, dual EP1 and EP3 selective antagonist based on a novel acyl sulfonamide bioisostere. *Bioorg Med Chem Lett* 2013;23:37–41. [PubMed: 23218714]
31. Ungerer M, Münch G: Novel antiplatelet drugs in clinical development. *Thromb Haemost* 2013;110:868–875. [PubMed: 24108565]
32. Alexander J, Chang GQ, Dourmashkin JT, Leibowitz SF: Distinct phenotypes of obesity-prone AKR/J, DBA/2J and C57BL/6J mice compared to control strains. *Int J Obes (Lond)* 2006;30:50–59. [PubMed: 16231032]
33. Nishikawa S, Doi K, Nakayama H, Uetsuka K: The effect of fasting on hepatic lipid accumulation and transcriptional regulation of lipid metabolism differs between C57BL/6J and BALB/cA mice fed a high-fat diet. *Toxicologic pathology* 2008;36:850–857. [PubMed: 18812581]
34. Nishikawa S, Yasoshima A, Doi K, Nakayama H, Uetsuka K: Involvement of sex, strain and age factors in high fat diet-induced obesity in C57BL/6J and BALB/cA mice. *Experimental animals / Japanese Association for Laboratory Animal Science* 2007;56:263–272.
35. Nishikawa S, Sugimoto J, Okada M, Sakairi T, Takagi S: Gene expression in livers of BALB/C and C57BL/6J mice fed a high-fat diet. *Toxicologic pathology* 2012;40:71–82. [PubMed: 22105644]
36. Legates JE: The role of maternal effects in animal breeding. IV. Maternal effects in laboratory species. *J Anim Sci* 1972;35:1294–1302. [PubMed: 4567217]
37. Mikami H, Onishi A: 'Heterosis' in litter size of chimaeric mice. *Genetical research* 1985;46:85–94. [PubMed: 4065568]
38. Rüllicke T, Guncz N, Wedekind C: Early maternal investment in mice: no evidence for compatible-genes sexual selection despite hybrid vigor. *Journal of evolutionary biology* 2006;19:922–928. [PubMed: 16674588]
39. Yan S, Tang J, Zhang Y, Wang Y, Zuo S, Shen Y, Zhang Q, Chen D, Yu Y, Wang K, Duan SZ, Yu Y: Prostaglandin E2 promotes hepatic bile acid synthesis by an E prostanoid receptor 3-mediated hepatocyte nuclear receptor 4 α /cholesterol 7 α -hydroxylase pathway in mice. *Hepatology* 2017;65:999–1014. [PubMed: 28039934]

Highlights

- DG-041 is a potent antagonist at the mouse EP3 receptor in vitro and in vivo.
- Subcutaneous administration of DG 041 achieves full coverage of EP3 in mice.
- Acute administration of DG-041 has no significant effect on body weight and glucose homeostasis.
- DG-041 blockade of EP3 suppressed lipid accretion in skeletal muscle.

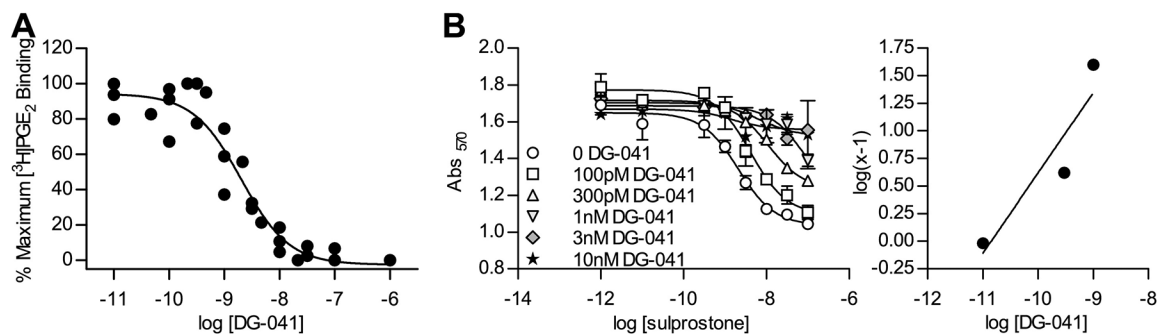


Figure 1. DG-041 is a high-affinity antagonist for the mouse EP3 receptor

A. Competition binding curve for DG-041 against 5 nM ^3H PGE₂ at the mouse EP3 γ receptor. Each data point is the average of triplicates and the data points are from three independent determinations. B. Schild analysis of DG-041 at HAmEP3 γ in LVIP2.0Zc cells (left). Concentration response curves to sulprostone in the presence of a range of concentrations of DG-041. Schild regression of concentration response data (right). Each point was determined in duplicate.

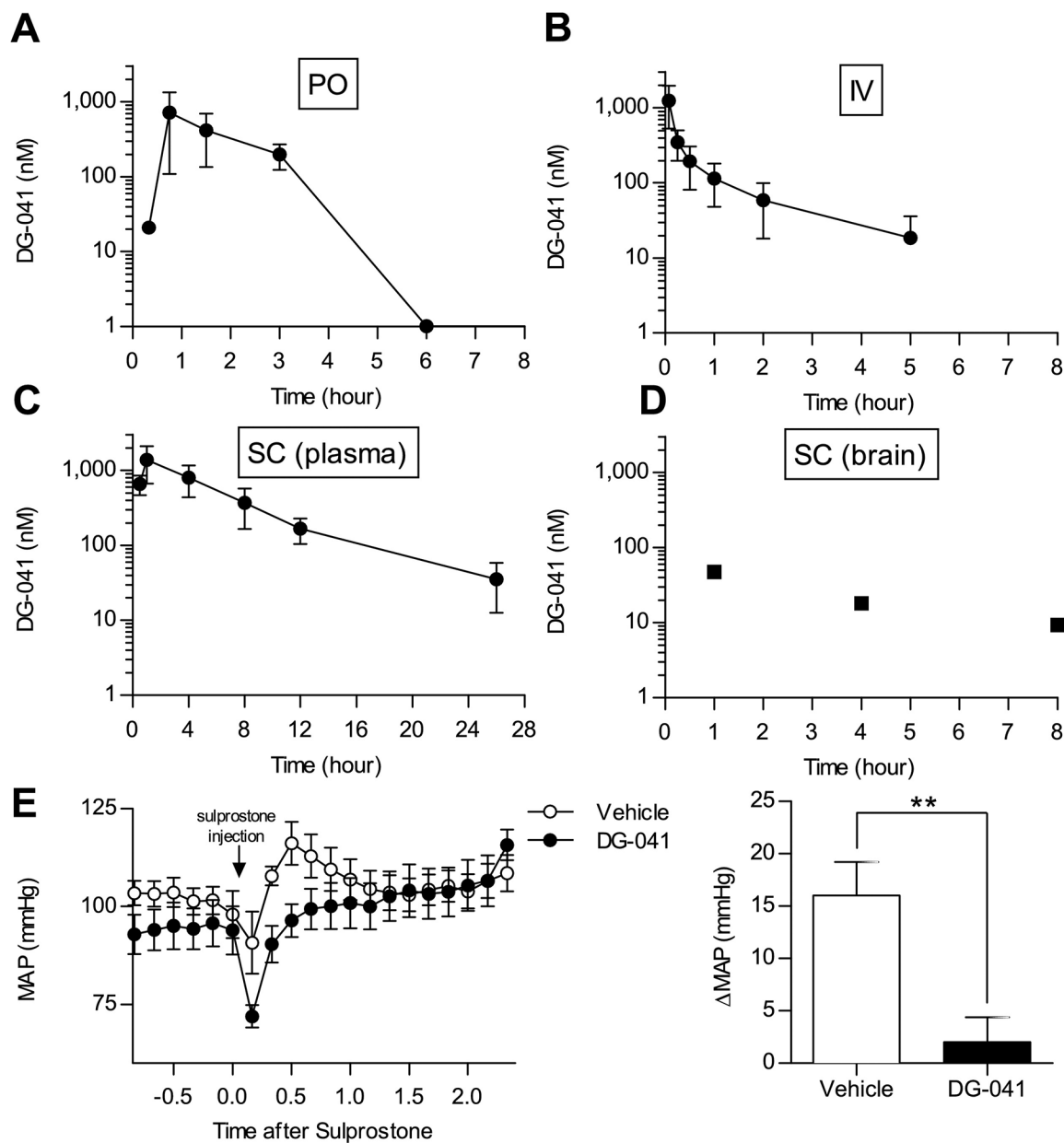


Figure 2. Plasma concentration-time profile of DG-041 following oral gavage, intravenous injection, and subcutaneous administration

A. 30 mg/kg DG-041 was administered to mice by oral gavage (*per os*, PO). Plasma DG-041 concentrations were measured from cardiac puncture blood. By six hours after gavage, plasma DG-041 concentrations were below the detectable limit. N = 2 mice per time point. B. 2 mg/kg DG-041 was administered by intravenous injection (IV). Plasma DG-041 concentrations were measured from saphenous vein or cardiac puncture blood at the indicated times. N = 5. C. 20 mg/kg DG-041 was administered to mice by subcutaneous injection (SC). Plasma DG-041 concentrations were measured from saphenous vein or cardiac puncture blood at the indicated times. N = 4–6. D. Brain DG-041 concentrations were measured from mice administered DG-041 via SC injection and euthanized at the

indicated time. E. Vehicle or 20 mg/kg DG-041 was administered by SC injection two hours before internal carotid blood pressure measurements. DG-041 treatment blocked the sulprostone-evoked rise in mean arterial pressure (MAP). N=5 each. For A–C values are expressed as mean \pm StDev, for D each data point is representative of one mouse, for E values are expressed as mean \pm SEM.

Author Manuscript

Author Manuscript

Author Manuscript

Author Manuscript

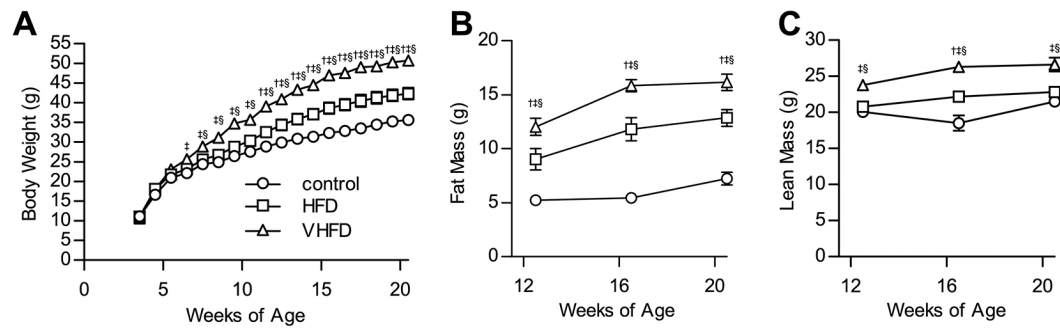


Figure 3. CB6F1 mice are obese when fed a HFD

A. Male mice fed control diet, HFD, or VHFD were weighed between 4 weeks of age and 20 weeks of age. After 3 weeks of VHFD feeding, mice were significantly heavier than mice fed control diet. By 4 weeks of VHFD feeding, mice were significantly heavier than mice fed HFD. At 8 weeks of HFD feeding, mice were significantly heavier than mice fed control diet. B. Body composition of fat was assessed by pulsed NMR. Fat mass in mice was increased by dietary fat and age ($P < 0.0001$). C. Body composition of lean mass was assessed by pulsed NMR. Lean mass in mice was increased by dietary fat and age ($P < 0.0001$). For Bonferroni post-hoc comparisons of $P < 0.05$: † control vs HFD, ‡ control vs VHFD, § HFD vs VHFD. For all figures $N = 8$ control, 8 HFD, 9 VHFD. Values are expressed as mean \pm SEM.

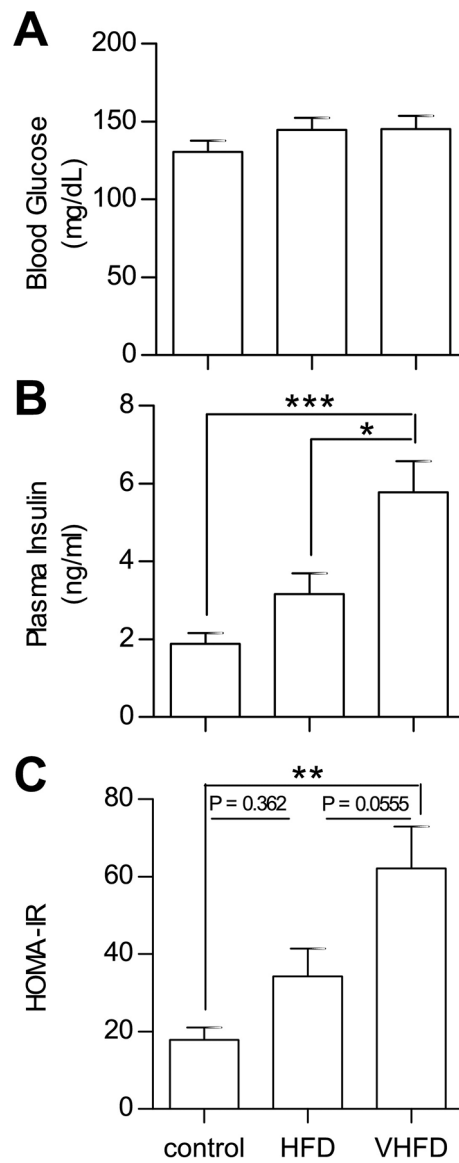


Figure 4. CB6F1 mice become hyperinsulinemic and insulin resistant when fed a HFD

The effects of dietary fat on insulin resistance was assessed in 20 week old CB6F1 mice. A. Dietary fat had no effect on blood glucose after a 6-hour fast ($P = 0.3653$). B. Increasing dietary fat increased fasting plasma insulin ($P = 0.0001$). C. The homeostatic model assessment of insulin resistance (HOMA-IR), a function of fasting blood glucose and plasma insulin, revealed that increasing dietary fat increased insulin resistance ($P = 0.0008$). For all figures $N = 8$ control, 8 HFD, 9 VHFD. Values are expressed as mean \pm SEM.

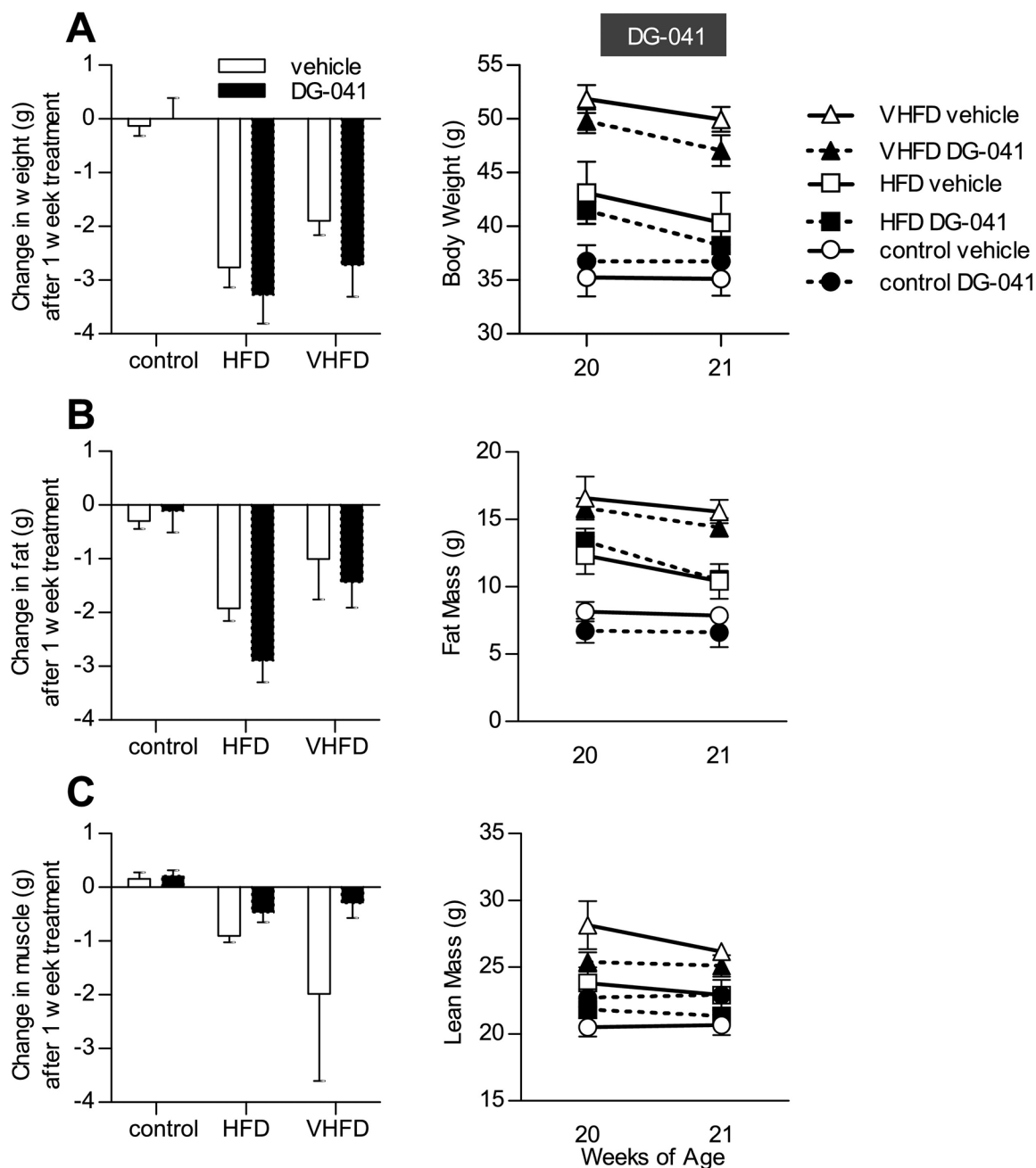


Figure 5. EP3 antagonist does not affect body composition

20 week old CB6F1 mice were administered DG-041 or vehicle by subcutaneous injection twice daily for one week. A. Administration of vehicle with or without DG-041 decreased body mass in mice fed HFD or VHFD ($P < 0.01$) but not in mice fed control diet ($P > 0.99$). DG-041 had a minimal effect on body weight as compared to vehicle in any dietary treatment group. B. Body composition of fat mass was assessed by pulsed NMR. DG-041 and vehicle treatment each decreased fat mass in mice fed HFD ($P < 0.01$) but not control diet ($P > 0.99$). In mice fed a VHFD, DG-041 decreased fat mass ($P = 0.0149$) but vehicle had no significant effect ($P = 0.2472$). DG-041 had a minimal effect on fat mass as

compared to vehicle in any dietary treatment group. C. Body composition of lean mass was assessed by pulsed NMR. Lean mass was not significantly affected by DG-041 or vehicle ($P > 0.99$ for all, except VHFD + vehicle $P = 0.0568$). DG-041 had a minimal effect on lean mass as compared to vehicle in any dietary treatment group. For all figures $N = 4$ control + vehicle, 3 control + DG-041, 4 HFD + vehicle, 4 HFD + DG-041, 4 VHFD + vehicle, 5 VHFD + DG-041. Values are expressed as mean \pm SEM.

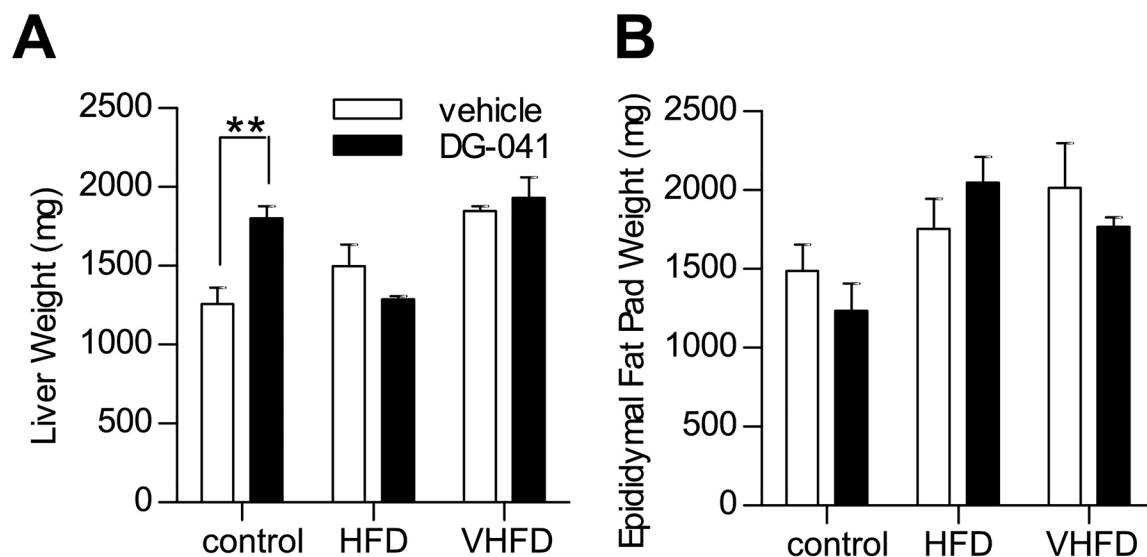


Figure 6. Liver and epididymal fat pad mass in mice treated with EP3 antagonist

The effect of EP3 antagonist, DG-041, on tissue weight was measured in 21 week old CB6F1 mice fed control, HFD, or VHFD. A. Increasing amounts of dietary fat increased liver mass in vehicle treated mice (One-way ANOVA test for linear trend, $P = 0.0094$). DG-041 did not have a significant effect on the weight of the liver (Two-way ANOVA effect of drug, $P = 0.0984$), except in mice fed control diet (post-hoc comparison, $P = 0.0047$). $N = 4$ control + vehicle, 3 control + DG-041, 4 HFD + vehicle, 4 HFD + DG-041, 4 VHFD + vehicle, 4 VHFD + DG-041. B. Dietary fat affected epididymal fat pad mass (Two-way ANOVA effect of diet, $P = 0.0142$). DG-041 did not significantly affect the weight of the epididymal fat pads (Two-way ANOVA effect of drug, $P = 0.6469$). $N = 4$ control + vehicle, 3 control + DG-041, 4 HFD + vehicle, 4 HFD + DG-041, 4 VHFD + vehicle, 5 VHFD + DG-041. Values are expressed as mean \pm SEM.

vehicle in any dietary treatment group. C. The homeostatic model assessment of insulin resistance (HOMA-IR), a function of fasting blood glucose and plasma insulin, demonstrated that overall treatment of the mice with vehicle with or without DG-041 showed a trend towards decreasing HOMA-IR ($P = 0.0158$), though no significant effect was observed under any individual condition ($P > 0.28$). DG-041 had a negligible effect on plasma insulin as compared to vehicle in any dietary treatment group. For all figures $N = 4$ control + vehicle, 3 control + DG-041, 4 HFD + vehicle, 4 HFD + DG-041, 4 VHFD + vehicle, 5 VHFD + DG-041. Values are expressed as mean \pm SEM.

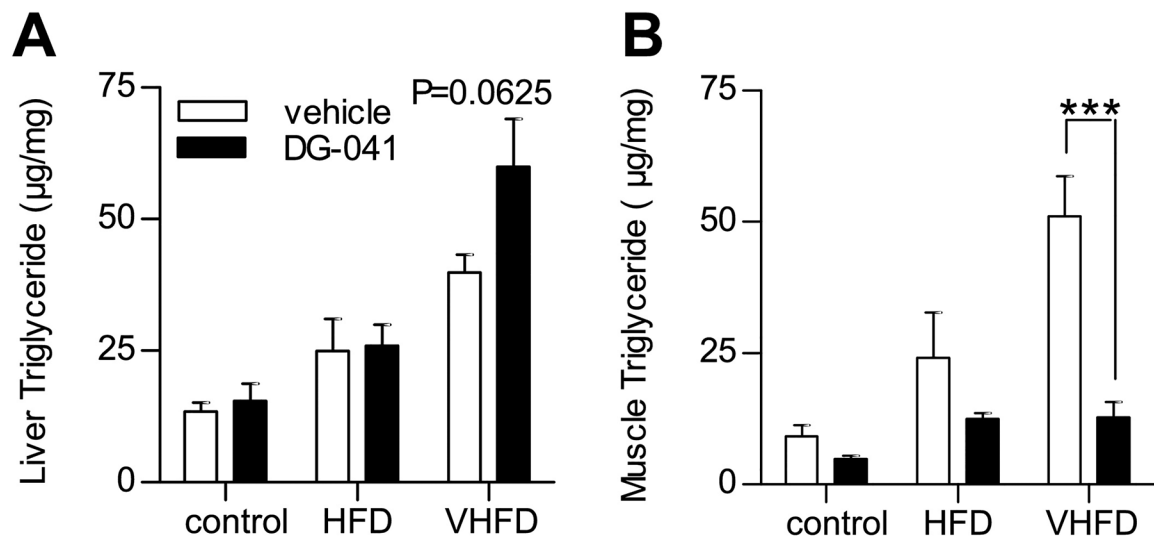


Figure 8. EP3 antagonist decreases skeletal muscle triglycerides

The effect of EP3 antagonist, DG-041, on triglyceride accumulation in ectopic tissues was measured in 21 week old CB6F1 mice fed control, HFD, or VHFD. A. Increasing amounts of dietary fat increased the amount of hepatic triglyceride ($P = 0.0234$). DG-041 did not significantly affect the amount of triglycerides in the liver ($P = 0.1321$). B. Dietary fat affected the amount of triglycerides found in the skeletal muscle ($P = 0.0005$). DG-041 significantly reduced the amount of triglycerides found in the skeletal muscle ($P = 0.0004$). For all figures $N = 4$ control + vehicle, 3 control + DG-041, 4 HFD + vehicle, 4 HFD + DG-041, 4 VHFD + vehicle, 5 VHFD + DG-041. Values are expressed as mean \pm SEM.

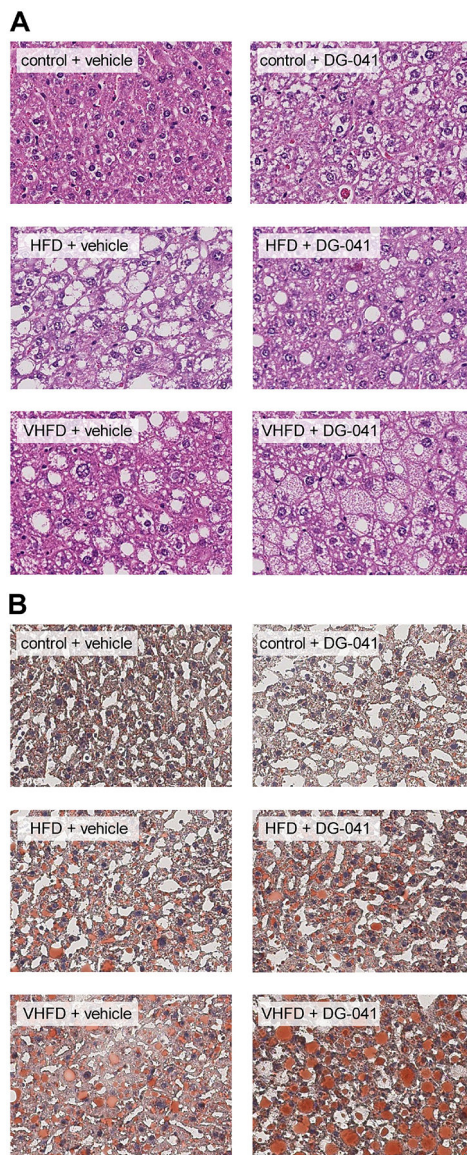


Figure 9. EP3 antagonist modestly increases hepatic lipid staining in mice fed VHFD

A. H&E staining of livers showed that dietary fat increased steatosis. No noticeable effect of DG-041 treatment on steatosis was observed. In VHFD mice treated with DG-041, hepatocellular ballooning was observed. B. Liver ORO staining was increased with increasing dietary fat. DG-041 appeared to increase ORO staining only in mice fed the VHFD. Images are a representative sample of sections from 4 control + vehicle, 3 control + DG-041, 3 HFD + vehicle, 4 HFD + DG-041, 4 VHFD + vehicle, 5 VHFD + DG-041.

Table 1.

Fatty acid composition of hepatic triglycerides

Fatty acid composition of hepatic triglycerides from male EP3^{+/+} and EP3^{-/-} mice, fed either HFD or control diet. N = 4 control + vehicle, 3 control + DG-041, 4 HFD + vehicle, 4 HFD + DG-041, 4 VHFD + vehicle, 5 VHFD + DG-041.

Parameter	control + vehicle		control + DG-041		HFD + vehicle		HFD + DG-041		VHFD + vehicle		VHFD + DG-041		ANOVA p-value		
	mean	SEM	mean	SEM	mean	SEM	mean	SEM	mean	SEM	mean	SEM	DG-041	Diet	Interaction
<i>g/100 g fatty acids</i>															
14:0	0.90	0.06	0.85	0.06	0.09	0.08	0.00	0.00	0.13	0.08	0.22	0.06	0.772	<0.001	0.335
16:0	25.14 ^{***}	0.31	28.81 ^{***}	0.77	24.35	0.64	23.68	0.29	26.10	0.28	26.15	0.42	0.015	<0.001	0.001
16:1	5.83	0.48	6.26	0.22	1.65	0.26	1.50	0.09	1.12	0.01	1.24	0.10	0.506	<0.001	0.523
17:0	0.00	0.00	0.00	0.00	0.00	0.00	0.00	0.00	0.00	0.00	0.00	0.00	NA	NA	NA
18:0	1.99	0.06	1.72	0.04	2.67	0.38	2.30	0.10	2.23	0.03	2.15	0.09	0.100	0.008	0.668
18:1ω9	43.14	1.05	44.96	1.58	35.74	1.62	36.74	0.18	32.68	0.35	35.23	0.53	0.038	<0.001	0.717
18:1ω7	6.90	0.42	7.01	0.08	1.83	0.22	1.79	0.09	1.34	0.04	1.41	0.09	0.781	<0.001	0.929
18:2	12.50 ^{**}	0.72	7.88 ^{**}	1.07	27.40	1.05	27.87	0.20	27.96 [*]	0.24	25.37 [*]	0.66	0.001	<0.001	0.009
18:3ω6	0.00	0.00	0.00	0.00	0.54	0.18	0.33	0.19	0.73	0.02	0.67	0.03	0.339	<0.001	0.633
18:3ω3	0.54	0.03	0.29	0.04	0.60	0.20	0.79	0.09	1.10	0.12	0.93	0.05	0.397	<0.001	0.123
20:3ω6	0.50	0.02	0.43	0.09	0.64	0.22	0.61	0.21	0.85	0.03	1.05	0.03	0.526	0.004	0.765
20:4	1.39 [*]	0.08	0.92 [*]	0.18	1.87	0.11	1.89	0.12	1.99	0.05	1.98	0.09	0.094	<0.001	0.060
20:5	0.00	0.00	0.00	0.00	0.00	0.00	0.00	0.00	0.06 [*]	0.06	0.20 [*]	0.05	0.154	0.002	0.123
22:4ω6	0.21	0.12	0.26	0.06	0.24	0.14	0.22	0.12	0.51	0.02	0.59	0.04	0.698	0.004	0.858
22:5ω6	0.19	0.11	0.10	0.10	0.16	0.09	0.00	0.00	0.15	0.09	0.16	0.07	0.287	0.592	0.573
22:5ω3	0.06	0.06	0.08	0.08	0.25	0.14	0.24	0.14	0.53	0.01	0.51	0.02	0.974	<0.001	0.976
22:6	0.71	0.11	0.44	0.14	1.99	0.20	2.05	0.07	2.54	0.05	2.14	0.12	0.065	<0.001	0.180
<i>Ratio</i>															
16:0/16:1	4.40 ^{***}	0.36	4.60 ^{***}	0.09	15.71	2.08	15.95	1.03	23.33	0.34	21.49	1.66	0.673	<0.001	0.656
18:0/18:1	0.04	0.00	0.03	0.00	0.07	0.01	0.06	0.00	0.07	0.00	0.06	0.00	0.007	<0.001	0.778
Saturated / Unsaturated [†]	0.39	0.00	0.46	0.02	0.37	0.01	0.35	0.01	0.40	0.00	0.40	0.01	0.034	<0.001	<0.001

[†] (14:0+16:0+17:0+18:0) / (16:1+18:1ω9+18:1ω7+18:2+18:3ω6+18:3ω3+20:3ω6+20:4+20:5+22:4ω6+22:5ω6+22:5ω3+22:6)

* Bonferroni post-hoc comparison P<0.05

Bonferroni post-hoc comparison $P < 0.01$
*
**

Bonferroni post-hoc comparison $P < 0.001$

Author Manuscript

Author Manuscript

Author Manuscript

Author Manuscript

Table 2.

Fatty acid composition of skeletal muscle triglycerides

Fatty acid composition of skeletal muscle triglycerides from male EP3^{+/+} and EP3^{-/-} mice, fed either HFD or control diet. N = 4 control + vehicle, 3 control + DG-041, 4 HFD + vehicle, 4 HFD + DG-041, 4 VHF + vehicle, 5 VHF + DG-041.

Parameter	control + vehicle		control + DG-041		HFD + vehicle		HFD + DG-041		VHF + vehicle		VHF + DG-041		ANOVA p-value		
	mean	SEM	mean	SEM	mean	SEM	mean	SEM	mean	SEM	mean	SEM	DG-041	Diet	Interaction
<i>g/100 g fatty acids</i>															
14:0	1.63	0.08	1.57	0.14	0.97	0.07	1.00	0.03	0.74	0.03	0.91	0.04	0.113	<0.001	0.015
16:0	16.86	0.78	17.94	0.79	17.24	0.85	17.15	0.59	17.11	0.41	18.24	0.98	0.038	0.453	0.228
16:1	18.53	0.84	17.60	2.01	7.15	0.53	7.48	0.90	4.88	0.49	5.93	0.44	0.692	<0.001	0.127
17:0	0.00	0.00	0.00	0.00	0.00	0.00	0.00	0.00	0.00	0.00	0.00	0.00	NA	NA	NA
18:0	1.18	0.23	1.27	0.24	2.58	0.23	2.62	0.36	3.24	0.10	3.02	0.18	0.737	<0.001	0.382
18:1 ω 9	42.05	0.59	41.99	1.81	47.25	0.92	47.33	0.28	50.00 [*]	0.54	46.78 [*]	0.73	0.008	<0.001	0.001
18:1 ω 7	4.42	0.26	4.44	0.18	1.88	0.22	2.12	0.21	1.46 ^{**}	0.15	2.29 ^{**}	0.33	0.002	<0.001	0.010
18:2	14.34	0.49	14.00	1.40	21.41	0.59	20.55	0.46	21.63	0.34	21.55	0.31	0.116	<0.001	0.455
18:3 ω 6	0.00	0.00	0.00	0.00	0.00	0.00	0.00	0.00	0.00	0.00	0.00	0.00	NA	NA	NA
18:3 ω 3	0.71	0.48	0.82	0.07	0.85	0.06	0.88	0.05	0.66	0.03	0.82	0.05	0.235	0.446	0.781
20:3 ω 6	0.00	0.00	0.00	0.00	0.13	0.09	0.19	0.01	0.11	0.01	0.03	0.08	0.720	<0.001	0.062
20:4	0.28	0.32	0.37	0.32	0.41	0.10	0.48	0.05	0.18	0.03	0.39	0.06	0.110	0.206	0.695
20:5	0.00	0.00	0.00	0.00	0.00	0.00	0.00	0.00	0.00	0.00	0.00	0.00	NA	NA	NA
22:4 ω 6	0.00	0.00	0.00	0.00	0.03	0.05	0.03	0.06	0.00	0.00	0.00	0.00	0.948	0.166	0.948
22:5 ω 6	0.00	0.00	0.00	0.00	0.00	0.00	0.00	0.00	0.00	0.00	0.00	0.00	NA	NA	NA
22:5 ω 3	0.00	0.00	0.00	0.00	0.00	0.00	0.00	0.00	0.00	0.00	0.00	0.00	NA	NA	NA
22:6	0.00	0.00	0.00	0.00	0.13	0.09	0.19	0.02	0.02	0.03	0.03	0.06	0.240	<0.001	0.458
<i>Ratio</i>															
16:0/16:1	0.91	0.08	1.03	0.08	2.43	0.24	2.33	0.38	3.54	0.49	3.10	0.39	0.310	<0.001	0.255
18:0/18:1	0.03	0.00	0.03	0.00	0.05	0.01	0.05	0.01	0.06	0.00	0.06	0.00	0.908	<0.001	0.822
Saturated / Unsaturated [†]	0.24	0.01	0.26	0.01	0.26	0.02	0.26	0.01	0.27	0.01	0.29	0.02	0.071	0.022	0.386

[†] (14:0+16:0+17:0+18:0) / (16:1+18:1 ω 9+18:1 ω 7+18:2+18:3 ω 6+18:3 ω 3+20:3 ω 6+20:4+20:5+22:4 ω 6+22:5 ω 6+22:5 ω 3+22:6)

^{*} Bonferroni post-hoc comparison P<0.05

Bonferroni post-hoc comparison $P < 0.01$
*
**

Bonferroni post-hoc comparison $P < 0.001$

Author Manuscript

Author Manuscript

Author Manuscript

Author Manuscript